Detector Perturbation of Ocean Radiance Measurements

Burns Macdonald 818 501 2505

Whitehead Associates
12012 Goshen Avenue, No. 311
Los Angeles, California 90049

William S. Helliwell

Science Applications International Corp.
10260 Campus Point Drive, MS-34
San Diego, California 92121

James Sanborn

Areté Associates
P. O. Box 6024
Sherman Oaks, California 91413

Kenneth J. Voss

Physics Department
University of Miami
Coral Gables, Florida 33124

ABSTRACT

The effect of a detector on the ocean radiance field being measured has been investigated - first, in a simple model whic accounts for perturbations in the radiance field introduced by the detector shadow and by light reflecting from the detector, an second, by a complete three-dimensional solution of the radiation transfer equation which calculates the perturbations by usin a computer model of a 4π radiance detection system (RADS[2]) with sky and ocean parameter choices to match California coast water. Results show that the presence of the detector has little influence on downwelling measurements nor do changes i detector reflectance. There is a substantial change due to the detector of upwelling radiance values. This may cause measure values to be reduced by as much as 30% below the unperturbed radiance for systems of the size of RADS (0.5 m) for ligh coming from the region of the detector shadow. The upwelling irradiance for this case is reduced 10%. Results are given fo sensors 0.5 m high and having diameters from 0.125 m to 2 m.

1. INTRODUCTION

Radiance distributions are the fundamental quantities for describing the optical properties of the oceans. Many othe quantities are reported in the literature including irradiance, water reflectivity and various attenuation coefficients that have bee measured either directly or indirectly. All of them could be derived from complete radiance distribution measurements Obtaining such measurements is a time consuming process that is hampered by numerous experimental difficulties Nevertheless, several experimenters have made sometimes extensive radiance measurements in various waters around the world An interesting survey together with related radiative transfer theory is presented in Reference 1. More recent radianc measurements have been made with an electro-optic ocean radiance distribution camera system (RADS)[2,3,4].

Care must be taken when deploying instruments from a surface ship to avoid the shadow cast by the ship. The ship shadow has an effect on radiance measurements to substantial depths. Even the cables used to support RADS affect the downwellin radiance distribution. The perturbation of the radiance by the cables appears very localized and is obvious in the data. A mor subtle effect may be in optical measurements that is due to the instrument. For example, the RADS system has physical scale

0-8194-0665-1/91/$4.

on the order of half a meter. Such an object will perturb the local radiance distribution, especially the upwelling radiance. The effect will not be as obvious as that of support cables on the downwelling radiance and could bias measurements without any distinctive indication in the data.

This paper analyzes numerical solutions to the radiative transfer equation to estimate the effect of an object on the radiance distribution in the ocean. The method of solution of the steady state radiative transfer equation in water has been developed for the radiance distribution (4π steradians) as a function of one space dimension - depth (1D), and for the radiance throughout an ocean volume (3D)[5,6,7,8]. This method uses various sky models and propagates the assumed input radiance through a smooth ocean surface and then through a chosen range of depths (1D) or throughout a volume of ocean (3D) using a given scattering phase function, an absorption coefficient, and a scattering coefficient, which all can vary with depth. Light scattering to all orders is calculated.

The 1D calculation models an ocean which does not change in the horizontal directions. The 3D method can model the radiance distribution which results when an underwater object perturbs the radiance field by absorption and reflection. A cylindrical model of the RADS system with parameter choices to match California coastal waters was used for the calculations presented in this paper.

2. SIMPLE MODEL

The perturbation in the radiance distribution is expected to be small for a typical camera system. Before generating full solutions of the radiance for various water optical parameters, a simple model will be developed that will be used to estimate reasonable parameter values that will give the largest radiance perturbations. Consider a plane at depth z with isotropic radiance specified at all locations (Fig. 1). The radiance has a constant value outside a disc of radius R at the coordinate system origin, $L^0(r,z,\phi,\theta) = L^0(r,z,0,\pi)$. In this notation z=0 at the surface and is positive upward, r is radial distance in a horizontal plane, ϕ is azimuth angle and θ is the polar zenith angle. The radiance is a specified constant value for $\theta \geq \pi/2$ and all φ. The disc is a Lambertian reflector with reflectivity r_d. The upward radiance at the center of the disc will be estimated.

The upward vertical radiance, L (r,z,0,0), due to an isotropic point source is proportional to a two-way point spread function f(r′) where r′ is the radial distance from the point source, $L(r',z,0,0) = f(r')\, L^0(r,z,0,\pi)$. The radiance at the center of the disc is the sum of all the radiance contributions from every point on the plane.

$$L^d(0,z,0,0) = 2\pi \int_0^R (L^d(r,z,0,\pi) - L^0(r,z,0,\pi))\, f(r)\, r\, dr + 2\pi \int_0^\infty L^0(r,z,0,\pi)\, f(r)\, r\, dr \qquad (1)$$

where $L^d(r,z,0,\pi)$ is the downwelling isotropic radiance at the disc. With no disc present the upward radiance is constant, $L^0(r,z,0,0) = r_w\, L^0(r,z,0,\pi)$, where r_w is the water reflectivity and the water is assumed to be a Lambertian reflector. Putting R=0 in Eq. (1) it is seen that the second integral on the right is equal to $L^0(r,z,0,0)$, and $r_w = 2\pi \int_0^\infty f(r)\, r\, dr$. To first order, i.e., neglecting shadow effects on the upwelling radiance distribution, the downward radiance at the disc is $L^d(r,z,0,\pi) = r_d\, L^0(r,z,0,0) = r_d\, r_w\, L^0(r,z,0,\pi)$. The perturbation in the upward radiance normalized by the unperturbed radiance is therefore

$$\left(\frac{\Delta L}{L^0}\right)_{up} \equiv \frac{L^d(0,z,0,0) - L^0(r,z,0,0)}{L^0(r,z,0,0)} = (r_d\, r_w - 1)\, \frac{\int_0^R f(r)\, r\, dr}{\int_0^\infty f(r)\, r\, dr} \qquad (2)$$

The first term on the right side ($r_d\, r_w$) is the extra upwelling radiance coming from upward light reflected down from the disc which is then backscattered onto the disc. The second term (-1) represents the loss of upwelling radiance which, in the absence of the disc, would have filled in its shadow and subsequently have been scattered back on to the bottom of the disc. Since water reflectivity is typically small, on the order of a few percent, and instrument reflectivity is typically around 10%, variations in the reflectivities r_w and r_d will have little effect on the normalized radiance perturbation.

Next consider the integral terms. If the radius of the disc is much less than the 3 dB radius of the two-way point sprea function then the effect of the disc is approximately proportional to its area. Once the radius of the disc is much larger tha the 3 dB radius, then further increases in the disc radius will have little effect on the upward radiance. Or looking at it fror the other direction, with a specified disc radius the water properties that will give the greatest effect are those where th two-way point spread function is narrower than the disc. This implies large absorption will produce a large effect.

The point spread function is also affected by the scattering phase function. The scattering properties of the ocean waters ar different at different locations and at different wavelengths. But the impact of the variations on the point spread function ar probably less than can be realized by variations in the absorption coefficient.

In order to obtain the normalized radiance perturbation accurately, the upward unperturbed radiance must be accurate. Thi means that it must be large enough to be observed reliably with a camera or to be calculated from a model with numeric accuracy. The implication is that the water reflectivity cannot be too small which in turn implies that the scattering coefficier cannot be too small.

The downward radiance at the top surface of the disc can be obtained in a similar fashion. Imagine an isotropic source L shining downward toward a plane with a disc. Such a radiance is a crude approximation to sky radiance.

The upward radiance (i.e., for $\theta < \pi/2$) that is reflected at the plane, assuming water is a Lambertian reflector, is given b

$$L^0(r,z,\phi,\theta) = L^0(r,z,0,0) = r_w L_s \tag{3}$$

A single scattering approximation for the total downward radiance (i.e., for $\theta > \pi/2$) at the plane is therefore

$$L^0(r,z,\phi,\theta) = L^0(r,z,0,\pi) = L_s + r_w L^0(r,z,0,0) = \left(1 + r_w^2\right) L_s \tag{4}$$

The upward radiance at the disc (assuming no interaction of the disc on the total downward radiance) is

$$L^d(r,z,\phi,\theta) = L^d(0,z,0,0) = r_d L^0(r,z,\phi,\theta) = r_d \left(1 + r_w^2\right) L_s \tag{5}$$

The downward radiance at the center of the disc is the sum of the downward radiance due to the sky and the upward radiance at all points in the plane

$$L^d(0,z,0,\pi) = L_s + 2\pi \int_0^R \left(L^d(r,z,0,0) - L^0(r,z,0,0)\right) f(r)\, r\, dr + 2\pi \int_0^{\infty} L^0(r,z,0,0)\, f(r)\, r\, dr \tag{6}$$

Using Eqs. (3), (4) and (5) this can be reduced to

$$\begin{aligned} L^d(0,z,0,\pi) &= L_s + \left(r_d \left(1 + r_w^2\right) - r_w\right) L_s\, 2\pi \int_0^R f(r)\, r\, dr + r_w L_s\, 2\pi \int_0^{\infty} f(r)\, r\, dr \\ &= \left(r_d \left(1 + r_w^2\right) - r_w\right) L_s\, 2\pi \int_0^R f(r)\, r\, dr + L^0(r,z,0,\pi) \end{aligned} \tag{7}$$

After rearranging Eq. (7) and using Eq. (4), the normalized perturbation in the downward radiance is

$$\frac{L^{d}(0,z,0,\pi) - L^{0}(r,z,0,\pi)}{L^{0}(r,z,0,\pi)} = \frac{\left(r_d - r_w + r_d\, r_w^2\right)}{1 + r_w^2}\, 2\pi \int_0^R f(r)\, r\, dr \tag{8}$$

Since r_w^2 is typically very small compared to one, and using the relationship between r_w and f(r), Eq. (8) is approximately

$$\left(\frac{\Delta L}{L^0}\right)_{dn} = \frac{L^{d}(0,z,0,\pi) - L^{0}(r,z,0,\pi)}{L^{0}(r,z,0,\pi)} = (r_d - r_w)\, r_w \frac{\int_0^R f(r)\, r\, dr}{\int_0^{\infty} f(r)\, r\, dr} \tag{9}$$

Analogous to Eq. (2), the term $r_d\, r_w$ represents the contribution to the downwelling radiance for light reflecting from the disc, while the r_w^2 term is the loss from upwelling light blocked off by the disc. For typical values of r_d and r_w the perturbation is only a few tenths of a percent.

The ratio of upwelling to downwelling normalized perturbations is, from Eqs. (2) and (9)

$$\frac{(\Delta L/L^0)_{up}}{(\Delta L/L^0)_{dn}} = \frac{r_d\, r_w - 1}{(r_d - r_w)\, r_w} \tag{10}$$

For values used here this ratio is about 500.

3. RADIATIVE TRANSFER

The radiance distribution L in a 3-dimensional scattering and absorbing medium satisfies the radiative transfer equation

$$\frac{dL}{ds} + c(\underline{x})\, L = \frac{b(\underline{x})}{4\pi} \int_{-\pi}^{\pi} \int_0^{\pi} p(\alpha)\, L(\underline{x}, \phi', \theta') \sin\theta'\, d\theta'\, d\phi' \tag{11}$$

Here, $\underline{x} = (x,y,z)$, z vertical, θ the polar zenith angle, and ϕ the azimuth angle. dL/ds is the directional derivative of L in the direction specified by (ϕ,θ). The function $c(\underline{x})$ is the attenuation coefficient, and $c(\underline{x}) = a(\underline{x}) + b(\underline{x})$, where $a(\underline{x})$ is the volume absorption coefficient and $b(\underline{x})$ is the volume scattering coefficient. In Eq. (11) we assume that any depth dependence in the volume scattering function can be factored out so that it is a product of $b(\underline{x})$ and the scattering phase function $p(\alpha)$. The scattering phase function here is only a function of the angle α between incident and scattered radiance directions, (ϕ,θ) and (ϕ',θ'), and is normalized so that its integral over 4π steradians solid angle is 4π. Any scattering phase function can be incorporated into the equation. The one we have used here is a curve fit to measurements reported by Petzold[9] for water off the California coast.

This equation is solved in water using a finite difference method with an iterative technique because of the scattering term on the right hand side. A fuller discussion of the solution of Eq. (6) is given in Ref. 7. In order to obtain a solution in the region of interest $\{x_{min} \le x \le x_{max},\ y_{min} \le y \le y_{max},\ z_{min} \le z \le 0\}$ radiance for all directions into the region must be specified at the boundaries.

These boundary values, involving incoming radiance only, are obtained from the 1D radiance transfer equation for the simpler problem where the radiance is uniform horizontally but still depends on depth and direction. At the surface (z=0) the in-water downwelling radiance is calculated starting, in this paper, from a clear-sky radiance distribution, a gaussian of 10° width. The peak value, in the sun direction, is normalized to one. The sky radiance is refracted through the (smooth) water surface. To

this is added the downwelling in-water radiance that is due to internally reflected radiance at the surface. Since the upwelling radiance that is reflected is not known beforehand the surface boundary downwelling radiance is coupled into the iteration scheme. At the maximum depth plane (z_{min}) incoming radiance is found assuming Lambertian reflection with reflectivity extrapolated from the water reflectivity of the neighboring depths. As at the surface, the incoming radiance depends on the solution and so is incorporated into the iteration scheme.

The 1D solution is used as the initial-guess input to the 3D code. For accuracy in the 3D finite difference solution the x,y,z grid points should be no further apart than one scattering length, 1/b. The choice of points for the present application is given in Figs. 2, 3, and 4. Depth planes are at 2.5 meter spacing. The angular grid points should be close enough so that the solid angle integration in Eq. (11) has the desired accuracy. In Fig. 4 the radius in the upwelling display represents zenith angles from 0° to 90° while in the downwelling display it represents angles from 180° to 90°.

Since the 3D radiance entering the sides of the ocean volume is fixed by the 1D solution the boundaries must be far enough away from the embedded object so that its influence on the radiance entering the boundaries is small. Experience with the model has shown that a distance of a couple of scattering lengths is sufficient.

Computer memory and time available to obtain a solution limits the actual number of points used in a 3D calculation. The solution time is directly proportional to the number of spatial grid points and to the square of the number of directions. External storage could have been used to permit larger array sizes but this has not been done. A solution with the grids used in this paper takes about half an hour on an Alliant FX/4 with one CPU. By contrast, 1D solutions take a few seconds on the same machine, or about 4 minutes on a 386-type personal computer. In all cases it takes about ten iterations for the radiance values to converge to better than 0.1%.

4. MODEL PARAMETERS

The camera sensor system is modeled as a cylindrical object inserted in the three-dimensional volume. Support cables are not included. The surface of the object is continuous and is defined independently of the radiance calculation grid. Grid planes are clustered in the region of the object so that rapid variations in the radiance near the object will be modeled well.

The cylinder is 0.5 meters in height which corresponds to the height of the RADS system as it was used in experiments conducted in 1987 and 1988[2]. Various diameters of the cylinder have been modeled: 0.5 m to correspond to RADS; 1.0 m and 2.0 m to increase the effect of the sensor on the radiance distribution and 0.25 m and 0.125 m to observe the behavior of the perturbed radiance as the diameter approaches zero. The sensor is inserted at a centerline depth of 15 m, and its surface is modeled as Lambertian with uniform reflectivity of 10%, corresponding to RADS.

The optical properties were chosen based on the results obtained from analysis of the simple model (Section 2). Moderate values of the absorption coefficient and water reflectivity are required. The conditions for a wavelength of 491 nm during the 1988 experiment[4] off the California coast seem appropriate. The total attenuation coefficient is modeled as a constant equal to 0.30 m^{-1} which corresponds to the data near 15-m depth. The scattering coefficient is obtained using the estimated value of the scattering albedo, b/c = 0.80. So b = 0.24 m^{-1}. The absorption coefficient is a = c - b = 0.06 m^{-1}.

5. MODEL RESULTS

Radiance distributions with no sensor in place (1D solution) are shown in Fig. 5. The downwelling radiance is at a depth of 14.745 m, 1/2 cm above where the top surface of the cylinder will be. The peak radiance corresponds to the sun direction which was 150° from vertical just beneath the ocean surface. The upwelling radiance is at a depth of 15.255 m, 1/2 cm below where the bottom surface of the cylinder will be. There is a weak but noticeable hump in the upwelling radiance in the sun plane, in the opposite direction to the peak sun radiance. This 180° scattering of the sun radiance is due to the backward peak in the scattering phase function for California coastal waters.

The influence of the sensor on the radiance distribution is shown by contour plots of the normalized perturbed radiance. This is the 3D radiance solution (with the sensor) minus the 1D radiance solution (without the sensor) divided by the 1D solution.

Normalized perturbed radiance distributions were calculated for all modeled sensors (0.5 m in height, 0.125 m to 2.0 m diameter, and with 10% reflectivity) 1/2 cm above and below the center of the sensor.

The downwelling radiance just above the sensor, in all cases, was perturbed by at most +0.6%, and rarely exceeded +0.2%. This downwelling data is not presented here because it was too close to the 0.1% iteration accuracy of the 3D calculations. Our simple model (Eq. 10) estimates that these values for downwelling radiance should be 500 times smaller than the upwelling perturbation values found below the sensor. This is in agreement in sign and approximate magnitude with the upwelling values reported below.

The upwelling radiance just below the 0.5 m diameter sensor was perturbed by 24% in the vertical direction and had a maximum value of 30% at 54° off the vertical (Fig. 6). In all cases, the radiance from the shadowed portion of the water is perturbed more than that from the non-shadowed water regions. Details of the perturbed radiance can be seen in Fig. 7 which shows cuts through the upwelling radiance contours of Fig. 6, both in the sun plane and perpendicular to the sun plane. The effects of light coming from the shadow area are apparent. The sharp rise near the end points is an artifact due to interpolating beyond 90° into the downwelling light region.

The effect of sensor size on the upwelling normalized perturbed light below the sensor is shown in Fig. 8 and in Table I, both for radiance in the vertical direction and for irradiance ($\int L \cos\theta \, d\Omega$). Since we kept the height of the cylinder constant while its diameter was varied we have used a composite area measure - the sensor's area, A_p, as projected on a horizontal plane along the sun direction. The straight line shown for the irradiance in the log-log plane has the form

$$\frac{-\Delta E}{E^0} = 0.137\, A_p^{0.30} \tag{12}$$

which fits the points with a standard deviation of 1.4%.

The reflectivity of the 0.5 m cylinder was changed from 0.10 to 0.027 which matched the water reflectivity at the sensor depth. The normalized perturbed irradiance went from -0.101 to -0.104, a decrease of 3%. The simple model (Eq. 2) predicts a decrease of only 0.2%.

Table I. Target-size dependence for upwelling light below the sensor of the normalized perturbed values for irradiance ($-\Delta E/E^0$) vertical radiance ($-\Delta L/L^0(0^0)$) and maximum radiance ($-\Delta L/L^0(\max)$). D - sensor diameter. Height is 0.5 m. A_p - sensor area as projected on a horizontal plane along the sun line.

D (m)	A_p (m^2)	$-\Delta E/E^0$	$-\Delta L/L^0$ (0^0)	$-\Delta L/L^0$ (max)
0.125	0.048	0.055	0.183	0.23
0.250	0.121	0.075	0.209	0.26
0.500	0.341	0.101	0.244	0.30
1.000	1.074	0.139	0.306	0.35
2.000	3.72	0.201	0.372	0.43

6. DISCUSSION

The 3D radiation transport calculations show that the downward radiance is not significantly affected for any sensor size used. Changes in sensor reflectivity also do not affect the downward radiance and these results are in general agreement with the predictions of the simple model. The upward radiance measurements by a camera system the size of RADS can, however, be substantially lower than the unperturbed radiance field, up to 30% for light coming from the direction of the detector shadow

and even more for larger sensors. The apparent saddle in the normalized upward radiance perturbations (Figs. 6 and 7a) is probably due to our interpolation scheme and to the lack of a grid point at $\phi = -90°$ in the region of $\theta = 30°$ (Fig. 4b). A simple peak here would indicate that the source of the perturbations is the ~180° backscattered light from direct rays of the sun that have been blocked by the senor.

The simple model shows the normalized radiance perturbations to be proportional to the sensor area for small sensors. The 3D model exhibits a dependence on sensor size which is considerably different (Eq. (12)) and which tends to zero much more slowly. This dependance of the 3D model is somewhat puzzling and the reasons for this are as yet unknown.

The simple model seems to give, qualitatively, the results found by the 3D calculations but there are many differences. It assumed a plane of isotropic sources where the 3D model used a gaussian sun source. It assumes the water is a Lambertian reflector, which is only approximately true. It does not include sensor shadow effects on the upward radiance, whereas the 3D model includes all scattering effects. The simple model can be substantially improved by incorporating more realistic radiance distributions to give values for normalized radiance perturbations but, because of the complexity of ocean radiance transmission, it would still be an approximate theory.

With further testing, the numerical solution of the 3D ocean radiance field would appear to be a useful tool to provide needed corrections to upwelling radiance measurements. This requires a geometric model of the sensor, knowledge of the ocean parameters a, b, and the scattering phase function, and a measurement of the downwelling radiance above the sensor. Corrections are expected to be especially important for sensors the size of submersibles and may be important in measurements made at all wavelengths in any ocean waters.

7. REFERENCES

1. K. Nygard, "Radiance distribution below the sea surface," in Optics of the Sea. AGARD Lecture Series No. 61 (1973).

2. K. J. Voss, "Radiance distribution measurements in coastal water," Ocean Optics IX, SPIE 925, 56-66 (1988).

3. K. J. Voss, "Electro-optic camera system for measurement of the underwater radiance distribution," Opt. Eng., 28, 241-247 (1989).

4. K. J. Voss, "Use of the radiance distribution to measure the optical absorption coefficient in the ocean," Limnol. and Oceanogr., 34, 1618-1626 (1989).

5. W. S. Helliwell and S. D. Gasster, "Obtaining inherent water optical properties from apparent water optical properties," Ocean Optics IX, SPIE 925, 14-21 (1988).

6. W. S. Helliwell, "Finite-difference solution to the radiative-transfer equation for in-water radiance," J. Opt. Soc. Am., 2 1325-1330 (1985).

7. W. S. Helliwell, G. N. Sullivan, B. Macdonald, and K. J. Voss, "A finite-difference discrete-ordinate solution to the three dimensional radiative transfer equation," J. of Transport Theory and Statistical Physics, 19, 333-355 (1990).

8. W. S. Helliwell, G. N. Sullivan, B. Macdonald, and K. J. Voss, "Ship shadowing: model and data comparisons," Ocean Optics X, SPIE 925, 55-71 (1990).

9. T. J. Petzold, "Volume scattering functions for selected ocean waters," Scripps Institute of Oceanography Visibility Laboratory, SIO Ref. 72-78, October (1972).

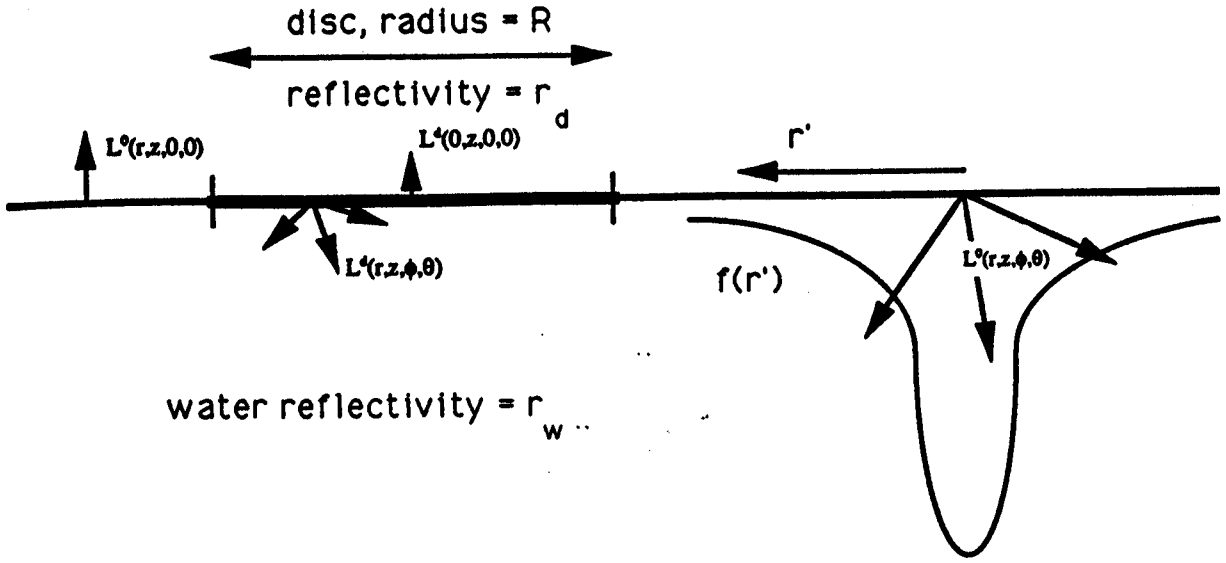

Fig. 1. Simple model geometry.

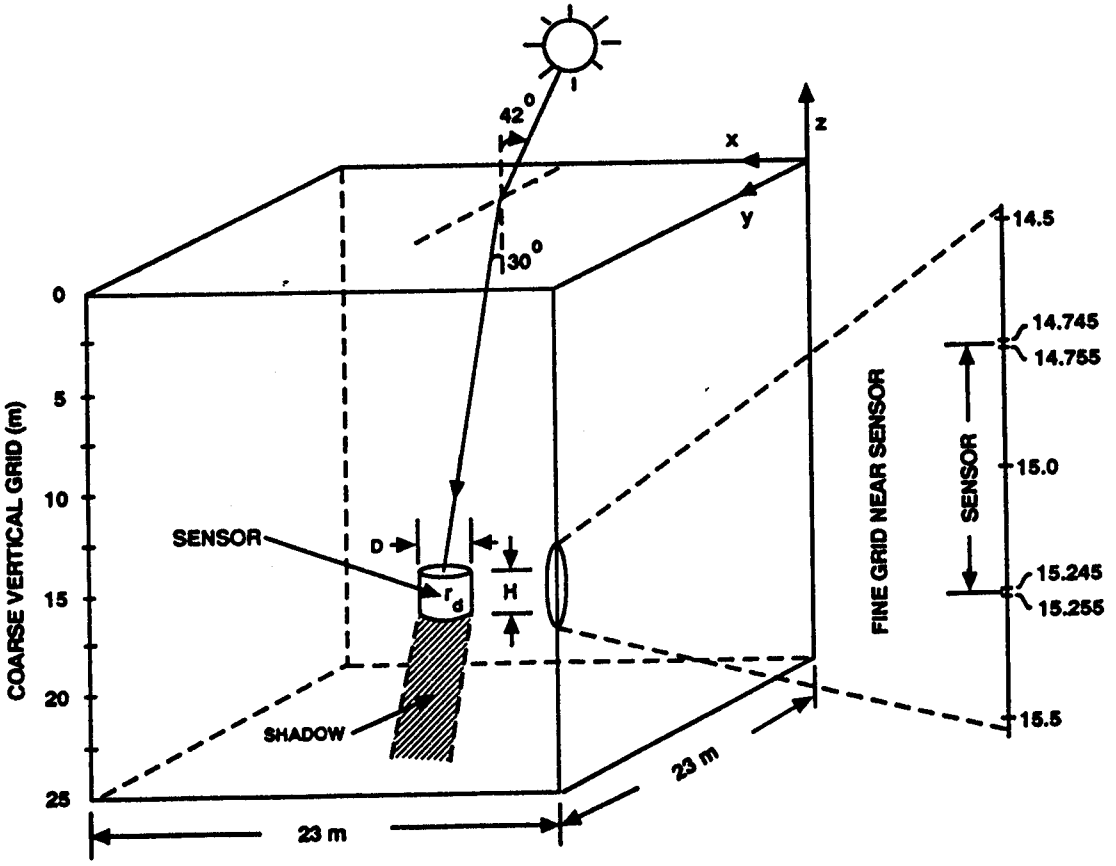

Fig. 2. Geometry of the radiance calculation showing the cylindrical sensor (height H, diameter D, Lambertian reflectivity r_d) centered at 15 m depth.

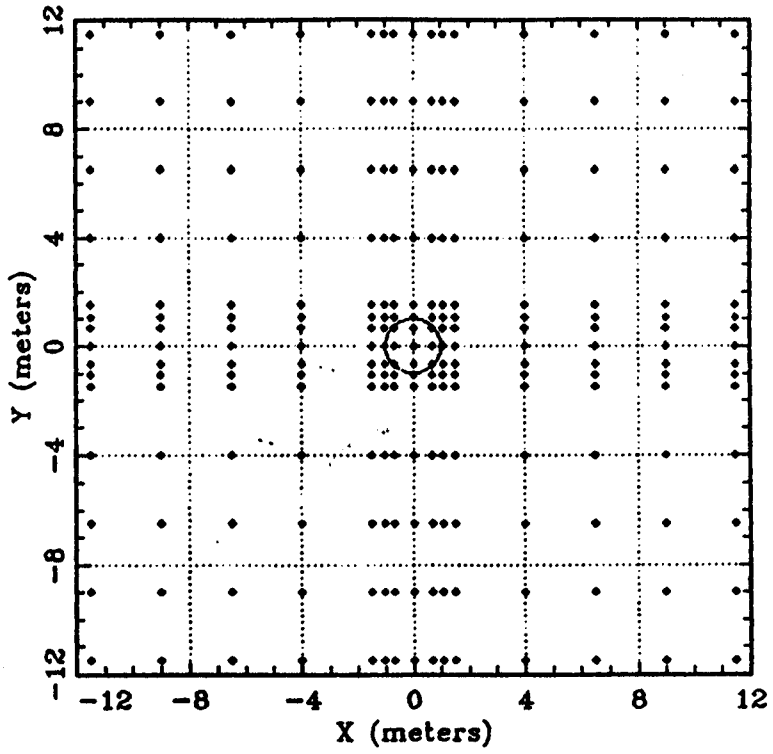

Fig. 3. The horizontal plane grid system used in the radiance calculations for the 2 m diameter sensor.

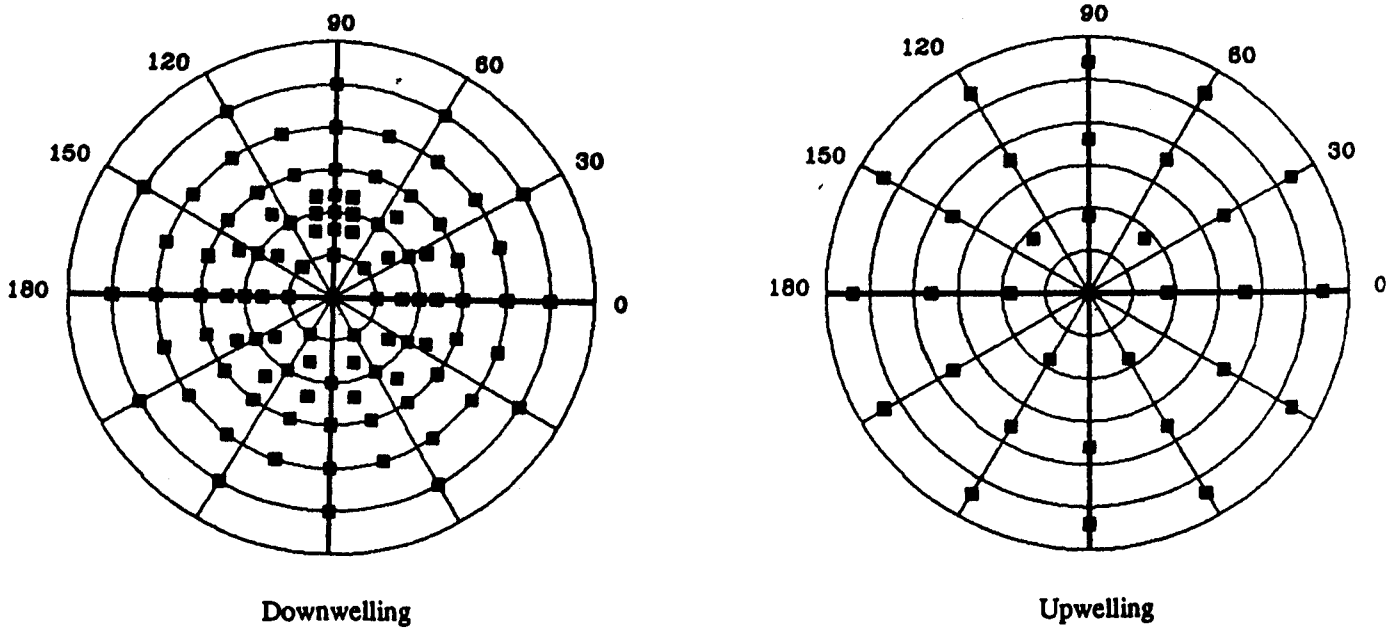

Downwelling

Upwelling

Fig. 4. Angles used by the 1D and 3D radiation transfer programs. Plotted radially (θ = 0° to 90°) is the nadir angle (downwelling) and zenith angle (upwelling).

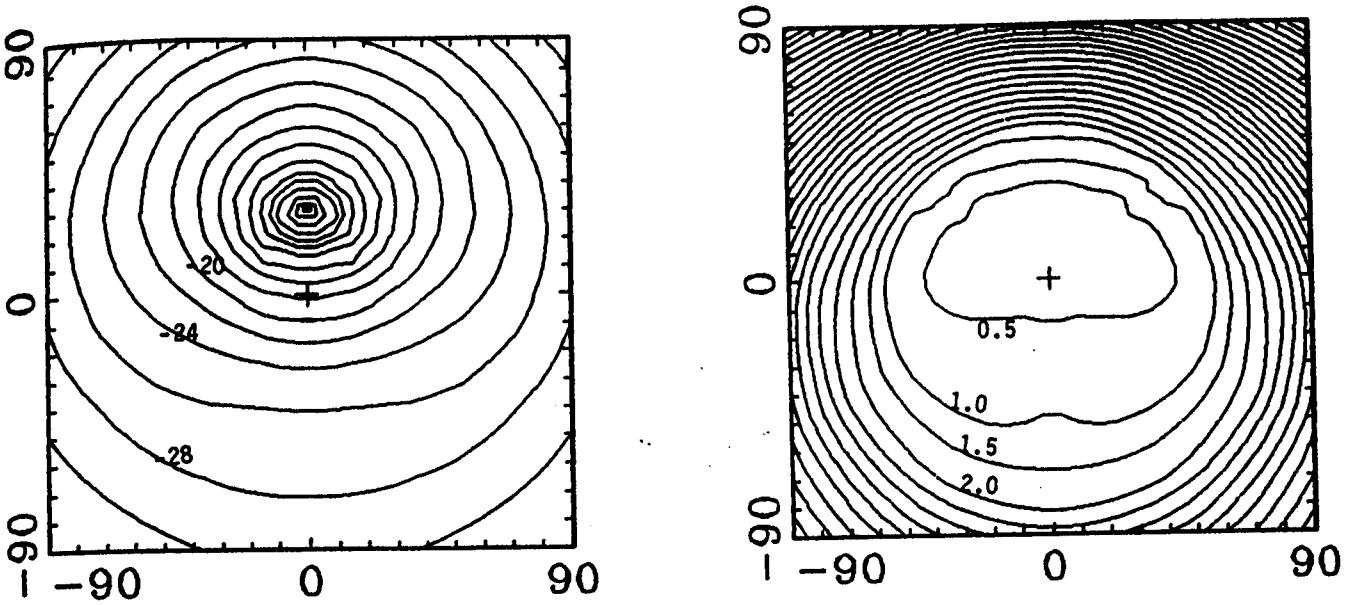

(a) Downwelling

(b) Upwelling

Fig. 5. Radiance distributions with no sensor in place at a depth (a) 1/2 cm above the position of the sensor top (z = -14.75 m) (downwelling radiance), and (b) 1/2 cm below the position of the sensor bottom (z = -15.25 m) (upwelling radiance). Contour levels are in dB below the maximum radiance (downwelling) and above the minimum radiance (upwelling).

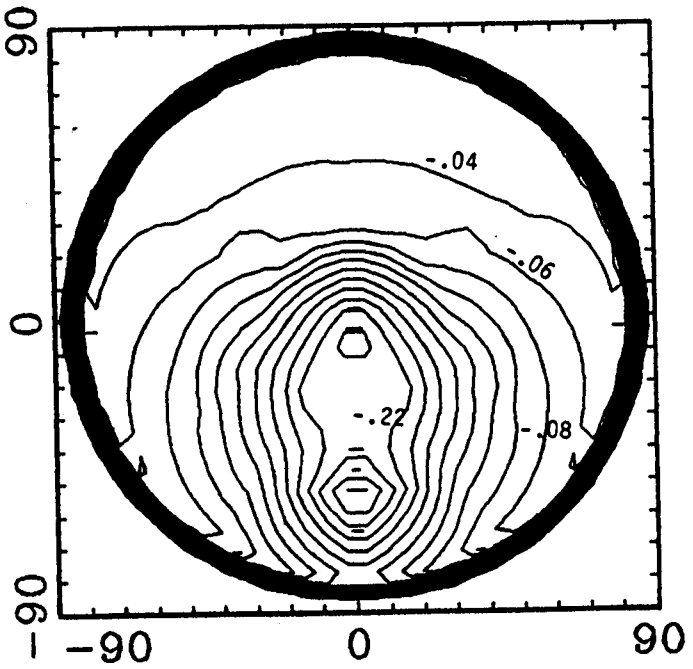

Fig. 6. The upwelling perturbed relative radiance $\Delta L/L^{\circ}$ just below the center of the sensor. Contour interval is 0.02.

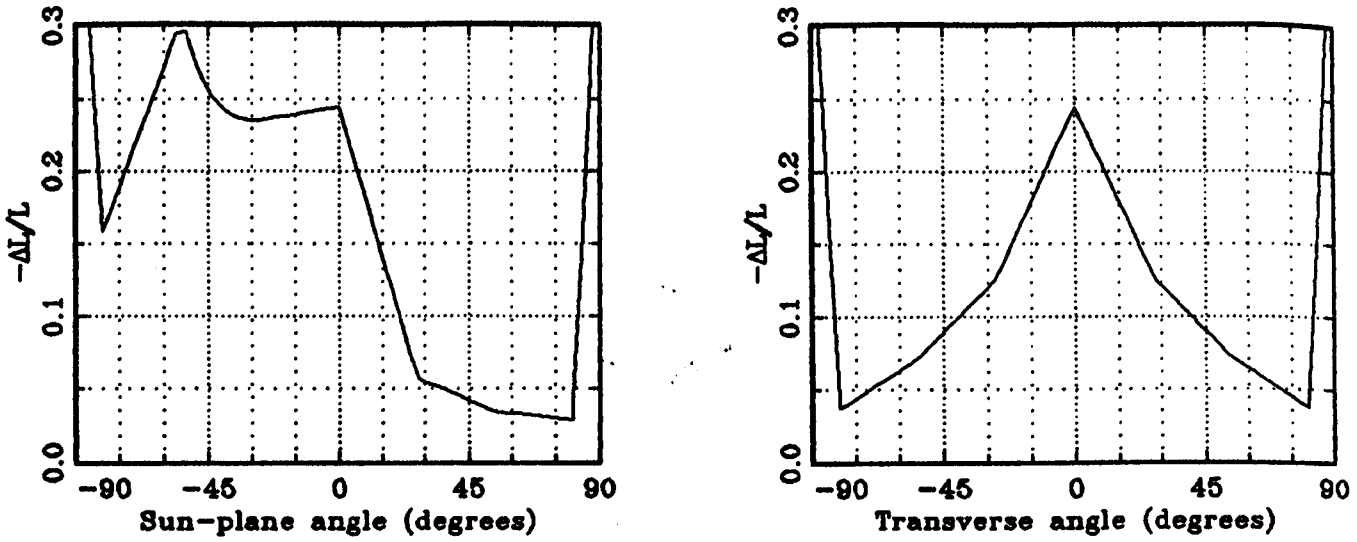

Fig. 7. The angular distribution ΔL/L° of Fig. 6 on a vertical line through the center (sun plane) and on the transverse line.

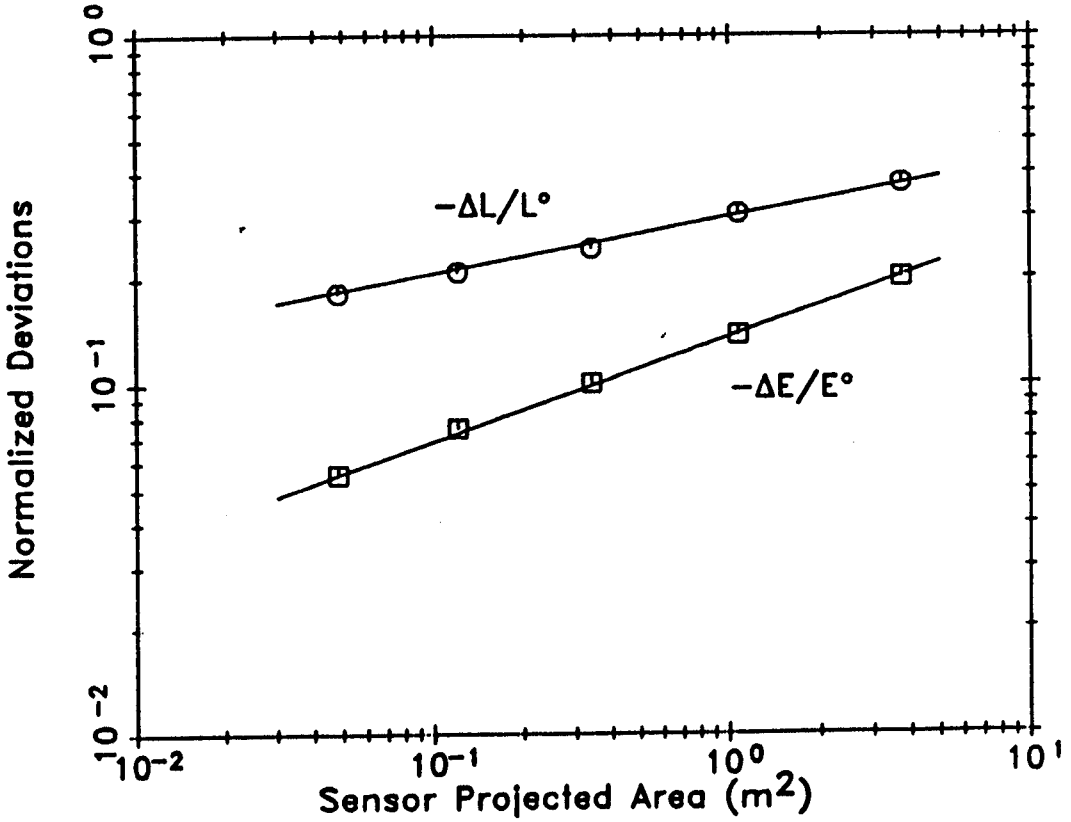

Fig. 8. For upwelling light just below the center of the sensor: the perturbed relative radiance ΔL/L° (θ=0) and irradiance ΔE/E° as a function of sensor area (as projected on a horizontal plane by the sun).